Proceedings of the ASME 2023 18th International Manufacturing Science and Engineering Conference
MSEC2023
June 12-16, 2023, New Brunswick, New Jersey

MSEC2023-104324

FLUID FLOW ANALYSIS FOR SUITABLE 3D BIO-PRINTED SCAFFOLD ARCHITECTURES TO INCUBATE IN A PERFUSION BIOREACTOR: A SIMULATION APPROACH

Scott Clark
Department of Sustainable Product Design and Architecture, Keene State College, Keene, NH.

Connor Quigley
Department of Sustainable Product Design and Architecture, Keene State College, Keene, NH.

Jack Mankowsky
Department of Sustainable Product Design and Architecture, Keene State College, Keene, NH.

MD Ahasan Habib*
Department of Sustainable Product Design and Architecture, Keene State College, Keene, NH.

ABSTRACT

Due to the three-dimensional nature of the 3D bio-printed scaffolds, typical stagnant cell culturing methods don't ensure entering medium inside areas or passing through the scaffolds. The bioreactor has frequently provided the required growth medium to encapsulated- and seeded- cells in 3D bio-printed scaffolds. To address this issue, we developed a customized perfusion bioreactor to supply the growth medium dynamically to the cells encapsulated or seeded in the scaffolds. The dynamic supply of fresh growth medium may help improve cell viability and proliferation. Because of its uniform nutrition distribution and flow-induced shear stress within the tissue-engineering scaffold, perfusion bioreactors have been used in a variety of tissue engineering applications. Including a modified setup of our designed bioreactor may improve the in vivo stimuli and conditions, eventually enhancing the overall performance of tissue regeneration. In this paper, we explored the response of fluid flow to certain types of scaffold pore geometries and porosities. We used a simulation technique to determine fluid flow turbulence through various pore geometries such as uniform triangular, square, diamond, circular, and honeycomb. We used variable pore sizes of the scaffold maintaining constant porosity to analyze the fluid flow. Based on the results, optimum designs for scaffolds were determined.

Key words: Bioreactor, Simulation, 3D Bioprinting, 3D Cell Culture.

1. INTRODUCTION

The goal of tissue engineering is to artificially regenerate organs or tissues to replace those that are diseased or damaged in the human body. Due to its multidisciplinary nature, which incorporates medicine, engineering, material sciences, chemistry, and biology, it attracts a lot of study attention in the goal of bridging the gap between organ shortage and transplantation necessity [1]. To create the engineered tissue scaffold, cells from the patient's blood or solid tissues can be employed directly, reducing the risk of immune system rejection and vaccination. The basic procedures in tissue engineering include cell extraction, 2D culture incubation and cell proliferation, engineered scaffold construction, cell maturation in the scaffold (i.e., tissue formation), and application. Therefore, it's important to choose a cell culture system [2] correctly. Static or traditional cell culture systems frequently don't seem to provide the necessary nourishment to enable tissue maturation and cell proliferation [3]. A bioreactor is crucial for accelerating cell growth by continuously supplying fresh growth medium [4, 5]. Perfusion bioreactors in particular enable dynamic fresh nutrients to flow axially through scaffolds that contain entirely natural stimuli that affect cell growth and differentiation [4]. A perfusion bioreactor has recently been developed to examine the mechanical properties and osteoblast responsiveness of bone scaffolds. [6]. A threefold perfusion bioreactor has reportedly been designed and manufactured to demonstrate a fully integrated organ bio-fabrication process. [7-9]. A new design of pulsatile bioreactor has been published for engineered aortic heart valve formation [10, 11].

To determine the effect of a 3D-scaffold architecture and related bioreactor process parameters, modeling and simulation of tissue-engineering systems are helpful [6]. Due to the inherent complex structure, it is challenging to attain internal information of 3D printed scaffold during incubation into the bioreactor. As an effort to identify that, a local volume average approach was used to evaluate the average shear stress in a porous media using required specific mathematical model [12]. However, this technique only resulted the average shear stress rather than overall distribution. In past years, the scaffolds were considered as impermeable structure in the development of fluid simulation models. The resulted simulation suggested an improved bioreactors and scaffold structures were identified [13]. To treat the inner structure and find the pore size and porosity as a repetitive patter of unit created by CAD model, some studies were reported [14]. The internal complex architectures were simplified by those studies. However, the demand for simulation on scaffolds having variational porosity along with the suitability of the bioreactor to incubate those scaffolds is increasing to analyze the fluid flow to observe the actual impact. Therefore, we studied simultaneously the design of bioreactor and scaffold geometry intending to perfuse growth medium with minimal turbulence.

Therefore, mathematical modeling and simulation techniques of the fluid dynamics in tissue growth process are helpful to investigate the flow distribution and nutrient transport in complex porous tissue scaffolds inside perfusion bioreactors [15]. Various simulation techniques were used to analyze the fluid flow and related impacts for perfusion bioreactor. A resolved scale numerical simulation was proposed to characterize the supply of glucose inside a porous tissue scaffold in a perfusion bioreactor, and to assess the overall culture condition and predict the cell growth rate [16]. To overcome the time-consuming trial and error experimental method, a computational fluid dynamics method was used is to design an optimized perfusion system [17]. Macroscale 3D printed vascular networks with various porosities were considered to predict the oxygen diffusion gradient using COMSOL model throughout the scaffold. Experimental work showed a cell viability increment up to 50% in the core of macroscale 3D printed vascular networks [18]. A computational evaluation was reported to assess fluid dynamics in 3D-printed scaffolds with different angular orientations between strands in each layer inside a perfusion bioreactor at different inlet flow rates [19]. Three flow rates such as 0.02, 0.1, and 0.5 ml/min were considered to simulate shear stress [20]. Not only flow rate, but the pore size also improves the cell growth such as a minimum pore sizes required for 3D bone regeneration range from 100 µm to more than 400 µm in the scaffold [21]. However, scaffolds having 800µm square pore size were reported to be used for bioreactor incubation [20]. To analyze the impact of fluid flow in a wide range, we considered the pore size from 500-2000 µm in this paper. In most of those papers, authors considered only regular square pore geometry with uniform size. In this paper, we considered triangular, square, and circular pore geometry along with uniform and variational pore sizes.

Recently we designed and developed a customized perfusion bioreactor to supply the growth medium dynamically to the cells encapsulated or seeded in the scaffolds [22] . The dynamic supply of fresh growth medium may help improve cell viability and proliferation. Because of its uniform nutrition distribution and flow-induced shear stress within the tissue-engineering scaffold, perfusion bioreactors have been used in a variety of tissue engineering applications. Including a modified setup of our designed bioreactor may improve the in vivo stimuli and conditions, eventually enhancing the overall performance of tissue regeneration. In this paper, we explored the response of fluid flow to certain types of scaffold pore geometries and porosities. We used a simulation technique to determine fluid flow turbulence through various pore geometries such as uniform triangular, square, diamond, circular, and honeycomb. This paper presents the preliminary analyses of fluid flow using a simulation technique. We used variable pore sizes of the scaffold maintaining constant porosity to analyze the fluid flow. Finally, bone tissue architecture was mimicked and simulated to identify the impact of fluid flow. Based on the results, optimum designs for scaffolds were determined.

2. MATERIALS AND METHODS

2.1 Description of our designed and manufactured perfusion bioreactor

The Bioreactor is comprised of five modules such as the Perfusion Chambers, the Medium Tanks, The Waste Port, The Oxygen Transfer, and The Perfusion Pump as shown in Figure 1. The control unit comprised Arduino and Breadboard controls various components around the bioreactor including solenoid pinch valves, micro vacuums, and liquid level sensors. The Arduino is connected to a power supply, micro stepper driver, and a circuit on a breadboard which allows for lower signals to be converted into higher voltages. Four output pins are connected to the microcontroller along with one input pin. The code runs on a main loop for a certain amount of time when tank 1 is full. If tank one is low, there will be a filling loop prior to the main loop based on the input of the liquid level sensor. After the main loop is finished, there is a waste loop that is performed to cycle away any unwanted cell waste. There are solenoid pinch valves between tank two and tank one, and between tank two and tank one to ensure medium cannot flow when it is not supposed to. The pinch valves are normally closed.

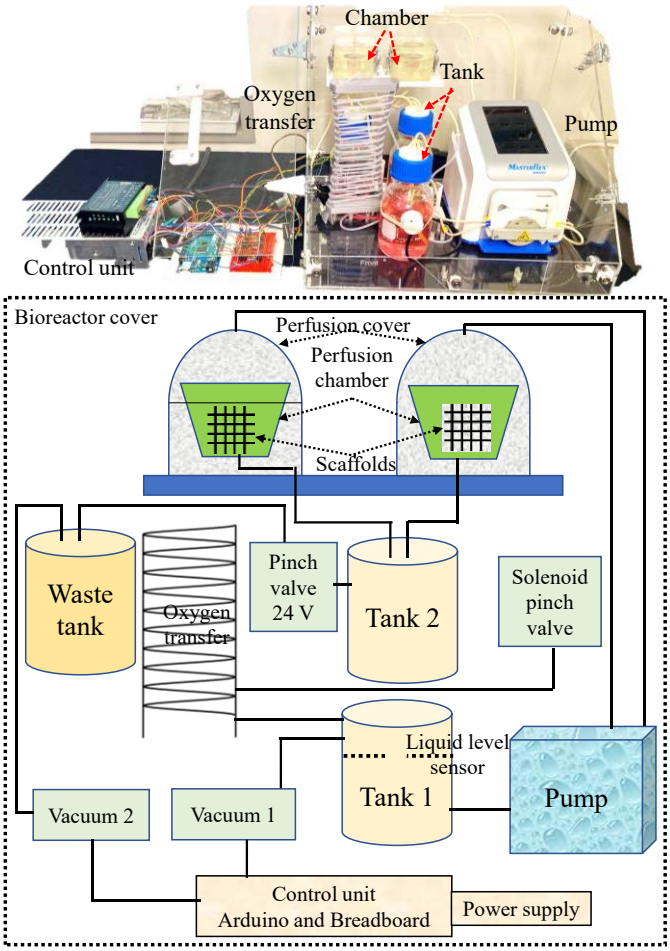

FIGURE 1: MODIFIED DESIGN OF BIOREACTOR CHAMBER COMPARED TO OUR PREVIOUS DESIGN

2.1.1 *Description of chamber*

Three factors have been considered in the design of the bioreactor's principal component, the chamber itself. The first requirement is that it must be a sealed environment that can hold the scaffold in place; this is required due to the sterility and growth media requirements for effective cellular cultures [23]. The second need is that the chamber must be modular or adaptable to allow the bioreactor to be used in more than one experiment. This is because previous bioreactor designs have the limitation of being able to only accommodate a particular type of scaffold [4, 5]. The chamber must guide flow through the scaffold rather than around it in order to enable for the flow of waste removal from the scaffold as well as the flow of nourishment and oxygen into the scaffold's inner sections [10].

Channel split into three near the end to reduce turbulence in the chamber as well as to minimize direct contact between the cells in the scaffold and the medium as shown in Figure 2(a). This internal geometry has stayed constant throughout all following iterations afterwards. Side latches were added on the sides instead of unscrewing four bolts to make it quicker and easier to open the chambers which was very tedious and time consuming off as shown in Figure 2(c).

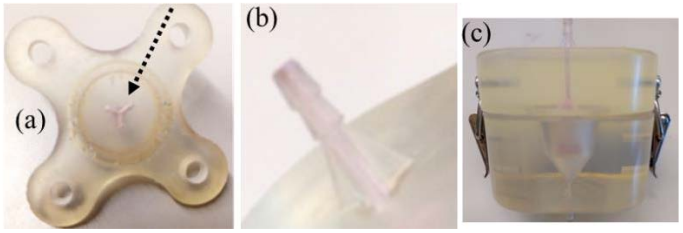

FIGURE 2: (a)THREE NEAR THE END SPLIT MAY REDUCE TURBULENCE IN THE CHAMBER, (b) THE ADDITION OF RIBS TO THE UPDATED CHAMBER ALLOWED TO POLISH WITHOUT THEM BREAKING OFF, AND (c) SIDE LATCHES WERE ADDED ON THE SIDES INSTEAD OF UNSCREWING FOUR BOLTS TO MAKE IT QUICKER AND EASIER TO OPEN.

2.1.2 *Perfusion cassette*

Our main chamber was designed as tapered for universal fit; the replaceable perfusion cassette can be made custom to the scaffold on hand regardless of its overall geometry so long as it fits within the volume of the main chamber as shown in Figure 3. Cassette with various internal geometries were modeled and fabricated using an SLA-based 3D printer, Form 3 (Formlabs, Somerville, MA) as shown in Figures 3. For simulation, we used the first model of Figure 3 in this paper as shown in Figure 4.

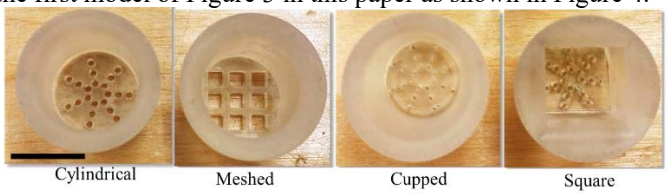

FIGURE 3: FABRICATED MODEL OF PERFUSION CASSETTES HAVING VARIOUS INTERNAL GEOMETRIES FOR VARIOUS SCAFFOLDS INCUBATION. SCALE BAR = 11 mm.

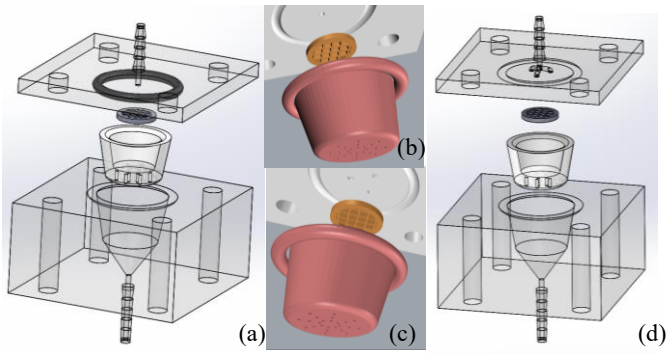

FIGURE 4: PREVIOUSLY DESIGNED (a) PERFUSION CHAMBER, (b) PERFUSION CHAMBER COVER; PROPOSED (c) PERFUSION CHAMBER COVER AND (d) PERFUSION CHAMBER.

2.2 Designing scaffold architecture

SOLIDWORKS (Dassault Systèmes SolidWorks Corporation, Waltham, MA), a Computer Aided Design (CAD) software was used to design a set of circular scaffolds having various internal architectures such as diamond, honeycomb, triangular, random circular, arranged circular, and square as shown in Figure 5. The diameter of the circle is 13 mm. The pore size of each scaffold was uniform. The porosities of those scaffolds were considered from 66.4% to 72.5%. We also generated scaffolds having variable pore sizes and geometries to analyze the impact of variational porosity on fluid flow during incubation in our bioreactor as shown in Figure 6(a-e). The porosity was varied from 56.43% to 70.79% depending on the internal pore sizes, geometries, and arrangement.

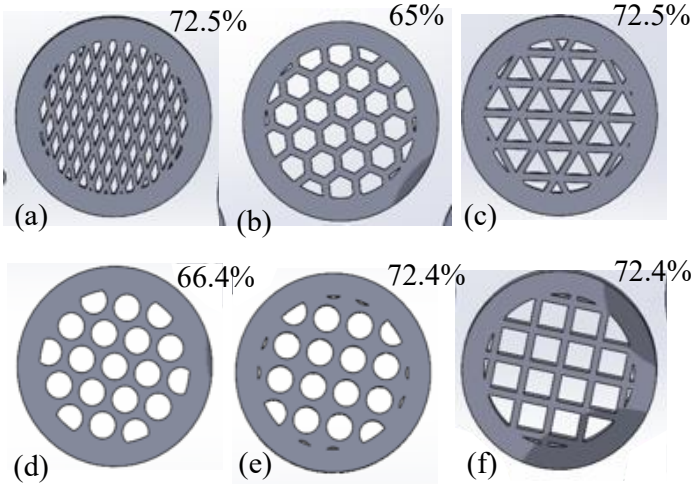

FIGURE 5: 3D MODELS USED FOR SIMULATION HAVING VARIOUS INTERNAL ARCHITECTUES: (a) DIAMOND, (b) HONEYCOMB, (c) TRIANGULAR, (d) RAMDOM CIRCULAR, (e) ARRANGED CIRCULAR, AND (f) SQUARES.

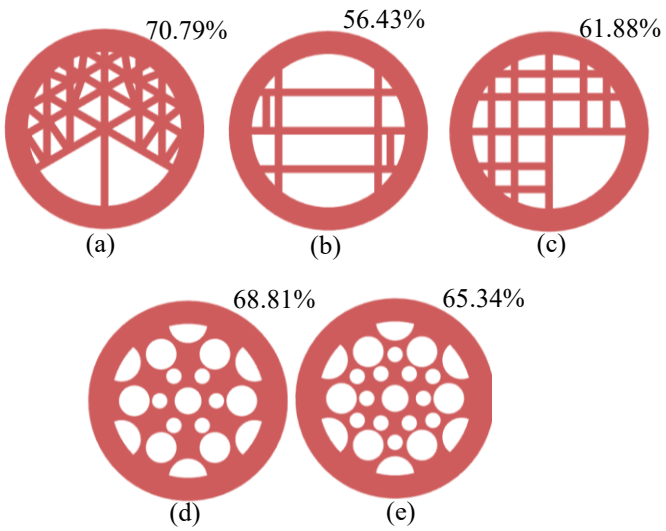

FIGURE 6: (a-e) 3D MODELS USED FOR SIMULATION HAVING VARIOUS INTERNAL ARCHITECTUES WITH VARIABLE PORE SIZES AND GEOMETRIES AND ARRANGEMENTS.

2.3 Flow simulation

SOLIDWORKS simulation package (Dassault Systèmes SolidWorks Corporation, Waltham, MA) was used to conduct all fluid flows. It is already reported that the scaffold geometries mainly control the selection of the optimal flow rates, under which the highest fraction of scaffold surface area is subjected to a wall shear stress that induces mineralization [24].

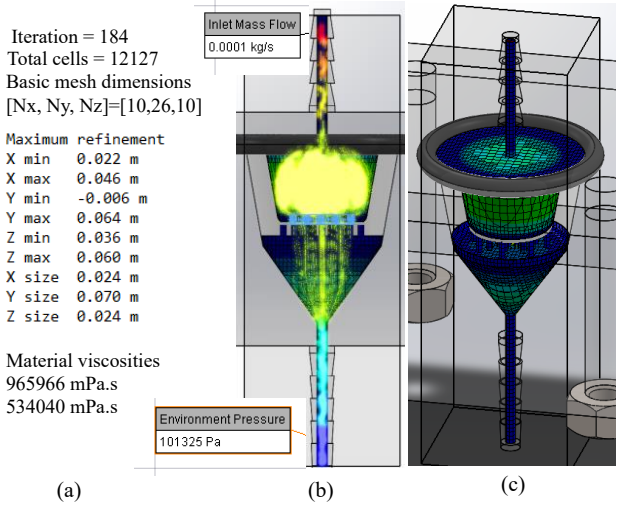

FIGURE 7: (a) SUMMARY OF THE BOUDARY CONDITIONS, (b) FLOW TRAJECTORY WITH SIMULATED RESULT, AND (C) MESH DISTRIBUTION OF THE SIMULATION.

However, the variation range of such optimal flow rates fall within 0.5–5 mL/min (or in terms of fluid velocity: 0.166–1.66 mm/s), among different scaffolds [24]. Since this paper aimed to conduct the simulation on scaffolds having various pore sizes and geometries, we considered a wide range of inlet masses such as 0.1g/s, 0.2g/s, 0.5g/s, and 1g/s and environmental pressures such as 101325 Pa, 151987 Pa, 202650 Pa, and 253312 Pa. A constant temperature of 20.15^{0}C was maintained throughout all simulation runs. We also compared the turbulence created by our previously designed perfusion cover with the redesigned one described in section 2.1.1. Two of our developed biomaterial compositions such as 4% Alginate(A) and 4% Carboxymethyl Cellulose (CMC, C) was used as scaffold material to conduct a real-world test. We will denote them as A_4C_4. The viscosities of A_4C_4 at 1.0 s^{-1} shear rate are 965966 mPa.s. A summary of boundary conditions of the simulations such as mesh size, total cell number, iteration, refinement factors, and so on along with the flow trajectory and mesh distribution is shown in Figure 7

2.4 3D printing of scaffolds

A composition comprised with 4% alginate and 4% Carboxymethyl Cellulose (CMC) (pH: 6.80) (Sigma-Aldrich, St. Louis, MO, USA) were prepared using our protocol used in our earlier work [25]. We used an extrusion-based 3D printer, BioX (CELLINK, Boston, MA) to release biomaterials layer-upon-layer and build scaffolds. Prepared hydrogels were loaded into 3.0 ml disposable barrel and released pneumatically on a building plat. A square scaffold (n=3) with 12 mm x 12 mm having a build height of 0.75 mm. The infill density for scaffolds was 7%. Various printing parameters such as nozzle diameter 250µm, print speed 5 mms^{-1}, layer height 0.25mm, and applied pressure 118-120 kPa were used to control the deposition rate of the hydrogels. These parameters were chosen to increase printability and pore size. The images of the deposited hydrogels and pore geometries at the same location were captured using the CK Olympus bright field microscope [26]. Rhino 6.0, a Computer-Aided Design (CAD) software, was used to design and define the vectorized toolpath of a scaffold. Slicer (https://www.slicer.org), a G-code generating program, was used to create a 3D printer-compatible file with the toolpath coordinates and all the process parameters needed to build the scaffolds. We confirmed the partial physical cross-link of the fabricated scaffold by spraying 4% (w/v) $CaCl_2$. Then, scaffold was placed into our custom-designed chamber and a fluid rate of 5ml/min was used as mentioned in other papers [24] as well.

3. RESULTS AND DISCUSSION

3.1 Simulation result for the scaffolds having uniform internal pore size and geometries.

The internal geometry of the scaffold that will house the cells in the bioreactor was tested in various configurations to find how it might affect the flow of the medium inside the bioreactor. The experiments were done using a flow simulation inside SolidWorks. The patterns that were tested were a grid-like pattern of squares, a pattern of circles arranged in a grid, a pattern of circles in a hexagonal arrangement similarly to a shower drain, a honeycomb-like pattern of hexagons, a pattern of rhombi, and a pattern of triangles. These scaffolds were also to test real-world viability. The simulations represent an ideal scenario, so by

printing the scaffolds at full size, 10mm in diameter, we could see which scaffolds are possible to make at this size. In future, we will print them in with appropriate hydrogels ensuring its internal architecture.

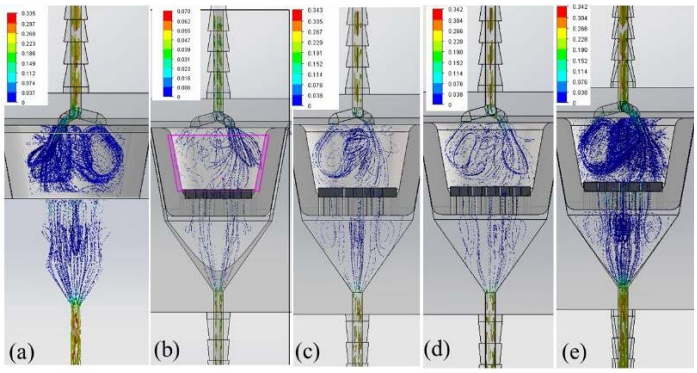

FIGURE 8: VELOCITY DISTRIBUTION INTO THE BIOREACTOR CHAMBER WHILE INCUBATED SCAFFOLD HAVING (a) TRIANGULAR, (b) SQUARE, (c) ARRANGED CIRCULAR, (d) RANDOM CIRCULAR, AND (e) HEXAGONAL PORES.

In the simulations, the pattern of triangles did not work well. Fluid was not able to flow through without adding more turbulence that could harm the cells as shown in Figure 9 (a). This pattern also showed 29% pore closure (7 out of 24 pores fully or partially closed), meaning pattern didn't print very well as shown in Figure 10 (a). From the velocity distribution as shown in Figure 8(a), fluid passes with high velocity (0.335 m/s) at the inlet and outlet of the chamber where the fluid flow rate into the chamber itself was minimal. The square pattern worked the best in all categories. It prints well (Figure 10 (b)) with 25% pore closure. It allows fluid to pass through and doesn't cause additional turbulence (Figures 8 and 10 (a)). Those results motivated us to use this pattern in the reactor for further experiments.

The circles arranged in a grid pattern worked better when than arranged in a hexagonal pattern since fluid seemed to flow through most of the pores in the grid pattern configuration whereas on the hexagonal pattern configuration it seems that the fluid wasn't flowing through the pores as evenly. The grid pattern had a 31% pore closure when printed, but the hexagonal pattern showed 47% pore closure. Both showed similar velocity. All those scenarios are shown in Figure 8-9 (c, d).

The honeycomb pattern, like the rhombi, didn't print well and showed 36% pore closure as shown in Figure 10 (e). The print also ended up looking more like circles than hexagons. It caused turbulence too close to the cells as shown in Figure 9(e). This pore geometry showed 0.342 m/s velocity. Table 1 showed a comparison of printability, % of pore closure, turbulence, and velocity at tip. From the velocity distribution, it is clear that the highest amount of turbulence was created by scaffolds having circular pore arranged either hexagonal or grid pattern and honeycomb pattern pores (0.343m/s). Scaffold having triangular pore showed 2.4% lower velocity at the entry and exit points compared to circular and hexagonal pores. Scaffold having square pores showed 390% and 378% lower velocity (0.07m/s) at the entry and exit points compared to circular and hexagonal pores and triangular pores respectively.

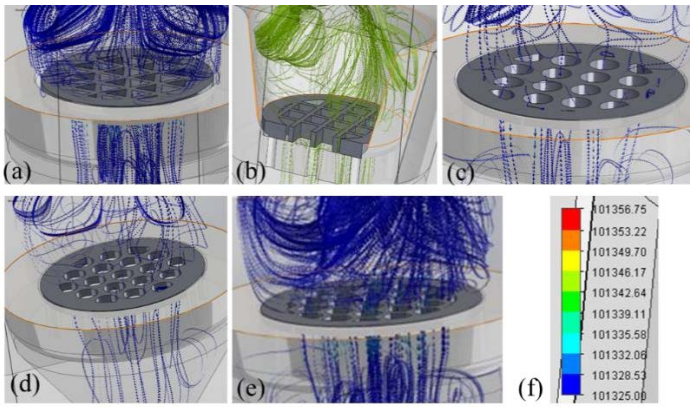

FIGURE 9: TURBULANCE CREATED BY THE SCAFFOLDS WHILE INCUBATED SCAFFOLD HAVING (a) TRIANGULAR, (b) SQUARE, (c) ARRANGED CIRCULAR, (d) RANDOM CIRCULAR, (e) HEXAGONAL PORES, AND (f) PRESSURE DISTRIBUTION.

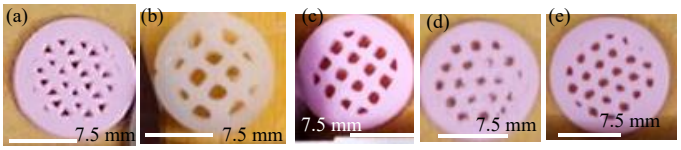

FIGURE 10: 3D PRINTED SCAFFOLDS HAVING: (a) TRIANGULAR, (b) SQUARE, (c) ARRANGED CIRCULAR, (d) RANDOM CIRCULAR, (e) HEXAGONAL PORES, AND (f) PRESSURE DISTRIBUTION.

Table 1: COMPARISON of RESULTS IN-TERMS OF PRINTABILITY (% OF PORE CLOSED), TURBULANCE, VELOCITY A TIP.

Pore geometries	% of pore closed	Turbulence	Velocity at tip (m/s)
Triangular	29	High	0.335
Square	25	Low	0.071
Arranged circular	31	Moderate	0.343
Random circular	47	Moderate	0.342
Honeycomb	36	High	0.342

3.2 Simulation result for the scaffolds having variational internal pore size and geometries.

Simulations were done to test internal scaffold geometry, similarly to the first simulations, but these scaffolds had pores of varying size to somewhat resemble organic tissue like bone

tissue where pores are not all the same size and neatly arranged. For these simulations, circles and squares were used since they worked best in the previous simulations. In neither of the arrangements with square/rectangular pores as shown in Figure 11 (a) and 11 (b) had any issues; however, since the medium is meant to contact the scaffold as it flows through in order to nourish the cells and remove waste, if the pores are too big, the medium was observed to pass through without touching the scaffold which defeats its purpose. Originally, only one scaffold with variational circular pores was modeled (Figure 11(c)). Since, the first had large sections of exposed surface area which led to more turbulence in the perfusion chamber, to resolve that issue, we modeled the second one as shown in Figure 11(d).

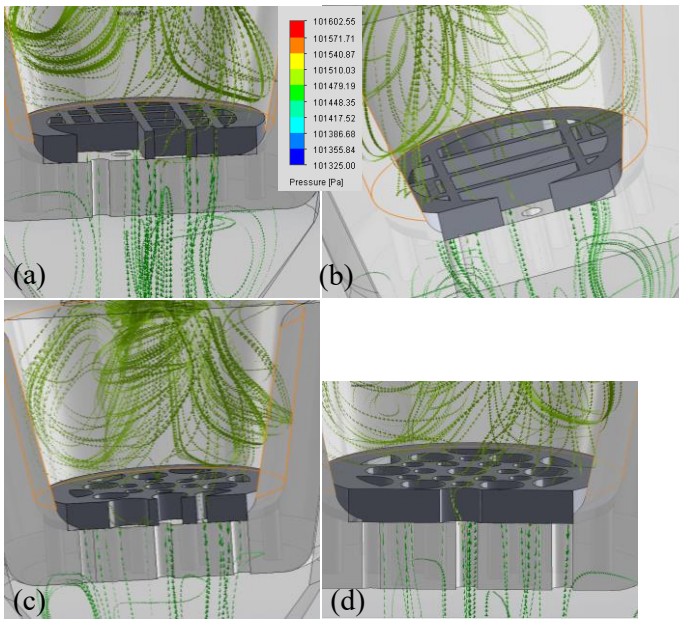

FIGURE 11: VELOCITY DISTRIBUTION INTO THE BIOREACTOR CHAMBER WHILE INCUBATED SCAFFOLD HAVING VARIOUS PORE SIZES AND GEOMETRIES.

We used the results from both sets of simulations and determine internal geometry of our scaffolds should look like. From the first, we decided that shapes that tessellate are best since they can be evenly distributed with a constant amount of surface area between them which can control the amount of turbulence. From the second, we found that the pores should be 1.50mm-2.0mm across so that the medium can flow through and contact the scaffold and that there should be 0.50mm-0.75mm in between each pore to avoid creating large areas of exposed surface area where the medium can bounce off. Using this data, we decided to use squares for the internal geometry of the scaffolds since they meet all our criteria.

3.3 Simulation result for smaller pore size

After finding that squares work best for pore shape in the 3D printed scaffolds, we simulated the fluid flow through smaller square pore expecting to see if the increased amount of exposed surface area would create unwanted turbulence in the perfusion chamber as seen in simulations with different shapes. The pores were 0.5mm by 0.5mm squares they were 0.5mm apart with a flow mass of 0.1, 0.2, 0.5, and 1.0 g/s. The velocity distribution for the mass flow of 0.1, 0.2, 0.5, and 1.0 g/s clearly indicates that higher mass flow will create more turbulence. The velocity of fluid flow through the entry and exit points of the chamber indicates a decreasing trend of the turbulence with increasing the flow mass. Therefore, it was showing 877% higher velocity (0.596mm/s) for a flow mass of 1.0 g/s compared to the flow mass of 0.1g/s (0.061mm/s) as shown in Figure 12.

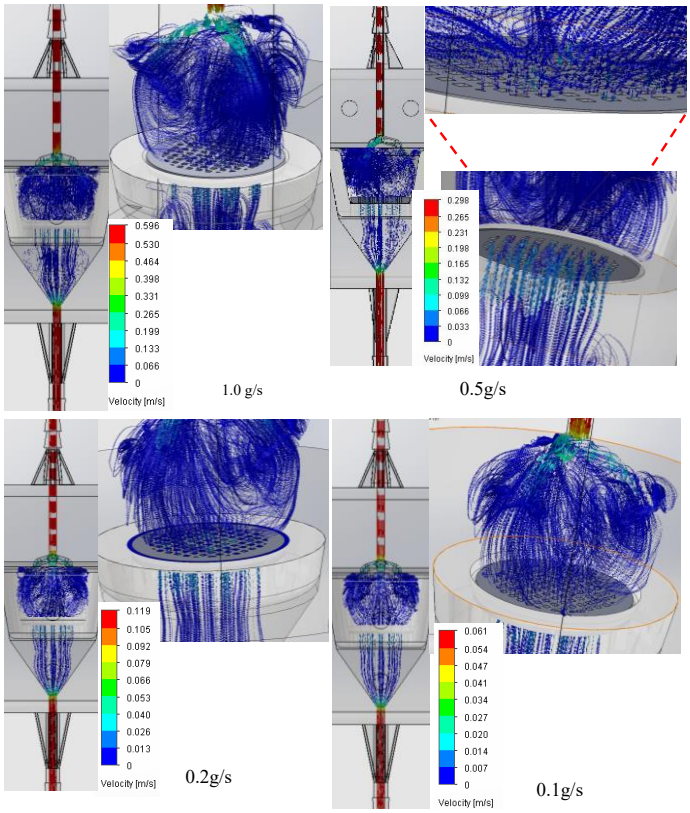

FIGURE 12: 3D MODEL WITH SMALLER PORE SIZES USED FOR SIMULATION HAVING VARIOUS MASS FLOW SUCH AS 0.1 G/S, 0.2 G/S, 0.5 G/S, AND 1.0 G/S

3.4 Test on printed scaffold

A new set of experiment was conducted for square-shaped scaffold. The swelling rate and percentage of material lost after 1, 2, 3, and 4 hours of incubation were determined. Same pore was captured to analyze the swelling rate. After completing each period of incubation (1, 2, 3, and 4 hours), material was dried to determine the percentage of material lost. Printed, submerged, and dried scaffold along with the pore geometry after the incubation of each period are shown in Figure 13.

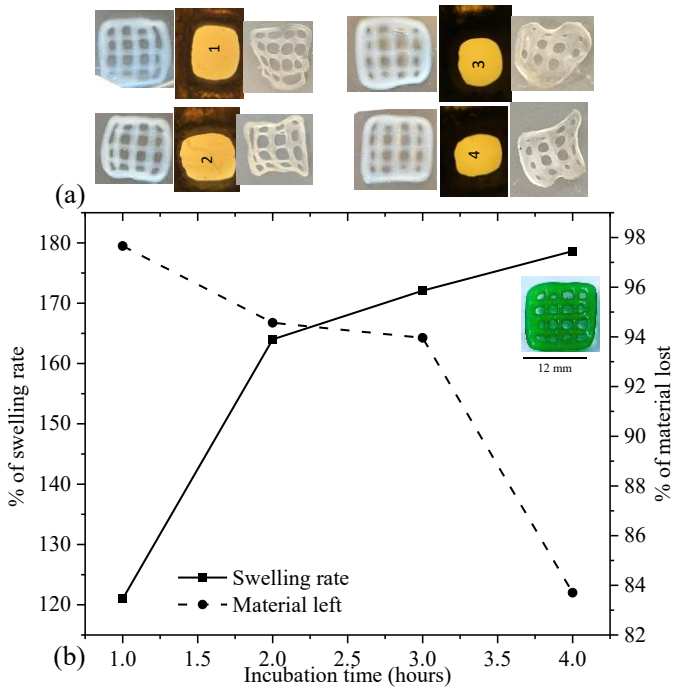

FIGURE 13: (a) SCAFFOLD SUBMERGED UNDER FLUID, MACRO-PORE GEOMETRY, AND DRIED SCAFFOLDS AND (b) % OF SWELLING RATE AND % OF MATERIAL LOST FABRICATED WITH A_4C_4. SCAFFOLD WITH GREEN COLOR WAS JUST AFTER THE PRINTING. THEN WE CROSSLINKED THE SCAFFOLD AND INCUBATED FOR 1, 2, 3, AND 4 HOURS. THE GEOMETRY OF PORE AFTER SWELLING WAS CAPTURED BY MICROSCOPE. FINALLY, WE DRIED THE SCAFFOLDS AFTER 1, 2, 3, AND 4 HOURS OF INCUBATION TO DETERMINE THE PERCENTAGE OF MATERIAL LOST DUE TO SWELLING.

4. CONCLUSION

In this paper, we demonstrated a simulation technique where the simulation test results can be used to determine the internal geometries effective for our custom-made perfusion chamber. This outlined technique can be utilized for other bioreactor chamber by adjusting process parameters of any specific perfusion bioreactor. Our first test result drove us to decide shapes that tessellate are best since they can be evenly distributed with a constant amount of surface area between them which can control the amount of turbulence. In addition to that, we found that the pores should be 1500 to 2000 µm across so that the medium can flow through. To confirm the contact of fluid flow with the scaffold, there should be 500-750 µm in between each pore to avoid creating large areas of exposed surface area where the medium can bounce off. Using this data, we prioritized the uniform internal pores as square, circular, triangular, and honeycomb to confirm effective fluid flow creating less turbulence. In future, we will fabricate scaffolds with various hydrogel developed in our earlier works [25, 27] conduct the fluid flow in the perfusion bioreactor designed and manufactured in our lab. Then, we will compare the actual fluid flow results with simulated test results. Afterward, we will move on to use our bioreactor to culture cells in the scaffolds. This will allow us to study the functionality of our scaffold designs, and lead to more research towards the development of creating viable three-dimensional scaffolds.

ACKNOWLEDGEMENTS

Research was supported by New Hampshire-EPSCoR through BioMade Award #1757371 from National Science Foundation and New Hampshire-INBRE through an Institutional Development Award (IDeA), P20GM103506, from the National Institute of General Medical Sciences of the NIH.

REFERENCES

[1] S. V. Murphy and A. Atala, "3D bioprinting of tissues and organs," *Nature biotechnology,* vol. 32, no. 8, pp. 773-785, 2014.

[2] M. Flaibani, C. Luni, E. Sbalchiero, and N. Elvassore, "Flow cytometric cell cycle analysis of muscle precursor cells cultured within 3D scaffolds in a perfusion bioreactor," *Biotechnology Progress,* vol. 25, no. 1, pp. 286-295, 2009/01/01 2009, doi: 10.1002/btpr.40.

[3] S. M. Mueller, S. Mizuno, L. C. Gerstenfeld, and J. Glowacki, "Medium Perfusion Enhances Osteogenesis by Murine Osteosarcoma Cells in Three-Dimensional Collagen Sponges," *Journal of Bone and Mineral Research,* vol. 14, no. 12, pp. 2118-2126, 1999.

[4] G. N. Bancroft, V. I. Sikavitsas, and A. G. Mikos, "Technical note: Design of a flow perfusion bioreactor system for bone tissue-engineering applications," *Tissue engineering,* vol. 9, no. 3, pp. 549-554, 2003.

[5] F. W. Janssen, J. Oostra, A. van Oorschot, and C. A. van Blitterswijk, "A perfusion bioreactor system capable of producing clinically relevant volumes of tissue-engineered bone: in vivo bone formation showing proof of concept," *Biomaterials,* vol. 27, no. 3, pp. 315-323, 2006.

[6] M. Bartnikowski, T. J. Klein, F. P. Melchels, and M. A. Woodruff, "Effects of scaffold architecture on mechanical characteristics and osteoblast response to static and perfusion bioreactor cultures," *Biotechnology and bioengineering,* vol. 111, no. 7, pp. 1440-1451, 2014.

[7] V. Mironov, V. Kasyanov, and R. R. Markwald, "Organ printing: from bioprinter to organ biofabrication line," *Current opinion in biotechnology,* vol. 22, no. 5, pp. 667-673, 2011.

[8] V. Mironov, V. Kasyanov, C. Drake, and R. R. Markwald, "Organ printing: promises and challenges," *Regenerative medicine,* vol. 3, no. 1, pp. 93-103, 2008.

[9] V. Mironov, R. P. Visconti, V. Kasyanov, G. Forgacs, C. J. Drake, and R. R. Markwald, "Organ printing: tissue spheroids as building blocks," *Biomaterials,* vol. 30, no. 12, pp. 2164-2174, 2009.

[10] S. P. Hoerstrup, R. Sodian, J. S. Sperling, J. P. Vacanti, and J. E. Mayer Jr, "New pulsatile bioreactor for in vitro

formation of tissue engineered heart valves," *Tissue engineering,* vol. 6, no. 1, pp. 75-79, 2000.
[11] K. Dumont *et al.*, "Design of a new pulsatile bioreactor for tissue engineered aortic heart valve formation," *Artificial organs,* vol. 26, no. 8, pp. 710-714, 2002.
[12] F. Boschetti, M. T. Raimondi, F. Migliavacca, and G. Dubini, "Prediction of the micro-fluid dynamic environment imposed to three-dimensional engineered cell systems in bioreactors," *Journal of biomechanics,* vol. 39, no. 3, pp. 418-425, 2006.
[13] E. M. Bueno, B. Bilgen, and G. A. Barabino, "Wavy-walled bioreactor supports increased cell proliferation and matrix deposition in engineered cartilage constructs," *Tissue engineering,* vol. 11, no. 11-12, pp. 1699-1709, 2005.
[14] M. T. Raimondi, F. Boschetti, L. Falcone, F. Migliavacca, A. Remuzzi, and G. Dubini, "The effect of media perfusion on three-dimensional cultures of human chondrocytes: Integration of experimental and computational approaches," *Biorheology,* vol. 41, pp. 401-410, 2004.
[15] D. W. Hutmacher and H. Singh, "Computational fluid dynamics for improved bioreactor design and 3D culture," *Trends in biotechnology,* vol. 26, no. 4, pp. 166-172, 2008.
[16] M. S. Hossain, D. Bergstrom, and X. Chen, "Modelling and simulation of the chondrocyte cell growth, glucose consumption and lactate production within a porous tissue scaffold inside a perfusion bioreactor," *Biotechnology Reports,* vol. 5, pp. 55-62, 2015.
[17] L. A. Hidalgo-Bastida, S. Thirunavukkarasu, S. Griffiths, S. H. Cartmell, and S. Naire, "Modeling and design of optimal flow perfusion bioreactors for tissue engineering applications," *Biotechnology and Bioengineering,* vol. 109, no. 4, pp. 1095-1099, 2012.
[18] O. Ball, B.-N. B. Nguyen, J. K. Placone, and J. P. Fisher, "3D printed vascular networks enhance viability in high-volume perfusion bioreactor," *Annals of biomedical engineering,* vol. 44, no. 12, pp. 3435-3445, 2016.
[19] A. R. Saatchi, H. Seddiqi, G. Amoabediny, M. N. Helder, B. Zandieh-Doulabi, and J. Klein-Nulend, "Computational fluid dynamics in 3D-printed scaffolds with different strand-orientation in perfusion bioreactors," *Iranian Journal of Chemistry and Chemical Engineering (IJCCE),* vol. 39, no. 5, pp. 307-320, 2020.
[20] H. Seddiqi *et al.*, "Inlet flow rate of perfusion bioreactors affects fluid flow dynamics, but not oxygen concentration in 3D-printed scaffolds for bone tissue engineering: Computational analysis and experimental validation," *Computers in Biology and Medicine,* vol. 124, p. 103826, 2020.
[21] I. Bružauskaitė, D. Bironaitė, E. Bagdonas, and E. Bernotienė, "Scaffolds and cells for tissue regeneration: different scaffold pore sizes—different cell effects," *Cytotechnology,* vol. 68, no. 3, pp. 355-369, 2016.
[22] A. Abbatiello and M. A. Habib, "Development of an In-House Customized Perfusion-Based Bioreactor for 3D Cell Culture," in *International Manufacturing Science and Engineering Conference*, 2022, vol. 85802: American Society of Mechanical Engineers, p. V001T01A016.
[23] I. Martin, D. Wendt, and M. Heberer, "The role of bioreactors in tissue engineering," *TRENDS in Biotechnology,* vol. 22, no. 2, pp. 80-86, 2004.
[24] F. Zhao, B. van Rietbergen, K. Ito, and S. Hofmann, "Flow rates in perfusion bioreactors to maximise mineralisation in bone tissue engineering in vitro," *Journal of Biomechanics,* vol. 79, pp. 232-237, 2018.
[25] A. Habib, V. Sathish, S. Mallik, and B. Khoda, "3D printability of alginate-carboxymethyl cellulose hydrogel," *Materials,* vol. 11, no. 3, p. 454, 2018.
[26] R. S. Kumar V, Cutkosky M, Dutta D, " Representation and processing heterogeneous objects for solid freeform fabrication," ed. Sixth IFIP WG 5.2 International Workshop on Geometric Modelling: Fundamentals and Applications, Tokyo, Japan, The University of Tokyo, 1998.
[27] C. Nelson, S. Tuladhar, L. Launen, and M. Habib, "3D Bio-Printability of Hybrid Pre-Crosslinked Hydrogels," *International Journal of Molecular Sciences,* vol. 22, no. 24, p. 13481, 2021.